Int. J. Electrochem. Sci., 15 **(2020)** 1287 – 1301, doi: 10.20964/2020.02.12

International Journal of
ELECTROCHEMICAL
SCIENCE
www.electrochemsci.org

Corrosion Inhibition Effect of Three Imidazolium Ionic Liquids On Carbon Steel In Chloride Contaminated Environment

Jingshun Cai[1,*], *Jiaping Liu*[2*], *Song Mu*[1], *Jianzhong Liu*[1], *Jinxiang Hong*[1], *Xiaochen Zhou*[1], *Qi Ma*[1], *Liang Shi*[1,3]

[1] State Key Laboratory of High Performance Civil Engineering Materials, Jiangsu Sobute New Materials Co., Ltd., Nanjing 211103 (P. R. China)
[2] Jiangsu Key Laboratory of Construction Materials, College of Materials Science and Engineering, Southeast University, Nanjing 211189 (P. R. China)
[3] Shanghai Suke Construction technology development Co. Ltd., Shanghai 201399 (P.R. China)
[*]E-mail: caijingshun@gmail.com, liujiaping@cnjsjk.cn

Received: 19 August 2019 / *Accepted:* 29 September 2019 / *Published:* 31 December 2019

Three imidazolium-type ionic liquids, substituted with polar groups at N1 and alkyl chains at N3 were synthesized under mild reaction conditions. The corrosion inhibition of carbon steel in 0.3 M NaCl saturated $Ca(OH)_2$ solution was investigated. Influence of concentration corrosion inhibition effectiveness was obtained by potentiodynamic polarization and electrochemical impedance spectroscopy. Imidazolium ionic liquid acted as a mixed type of inhibitor by both chemical and physical adsorption on the steel surface in terms of the Langmuir adsorption isotherm. All ionic liquids showed appreciable inhibition efficiency, and the relationship between chemical structure and inhibition activity was revealed. Surface analysis suggested that imidazolium ionic liquids could effectively inhibit the formation of corrosion products.

Keywords: carbon steel; corrosion inhibitor; imidazolium ionic liquid; synthesis

1. INTRODUCTION

Corrosion of steel reinforcement in concrete had been considered as a major cause for concrete deterioration. According to statistics, the total value of $6 trillion of reinforced concrete buildings in United States, because of steel corrosion caused by the reconstruction and maintenance costs hundreds of billions of dollars every year. There are more and more reinforcement concrete construction suffer from steel corrosion. In order to repair the corrosion damage of reinforced concrete, several methods were proposed and developed, such as, electrochemical chloride extraction, migrating corrosion inhibitor, sealing and membranes for concrete surface. Due to the low cost and easy-operation, migrating corrosion inhibitor were widely studied and applied for corrosion of steel repair[1].

The typical migrating corrosion inhibitors widely studied are mainly based on amines and alkanolamines, thanks to their relatively high vapour pressure[2-5]. However, the ability of these inhibitors to penetrate into concrete greatly depends on the cover depth and permeability of the concrete[6]. To overcome the present limitations, a new technique called electrical injection of corrosion inhibitors (EICI) was developed, in which the positively-changed inhibitors could be driven to the steel surface by an externally applied electric field[7]. Several organic inhibitors with specific chemical structures as shown in Fig. 1, have been investigated in laboratory studies to date. Page. reported cationic conjugate acid type inhibitors which were formed by protonation of organic bases, such as ethanolamine and guanidine[6, 8, 9]. Very recently, another cationic conjugate acid type inhibitor, protonated triethylenetetramine (TETA) was studied in chloride contaminated concrete[10]. Notably, EICI has been little explored for practical application. The only well known example was reported by Kubo, in which ethanolamine was protonated and eletro-injected to alleviate reinforcement corrosion for a 40-year-old carbonated high-speed railway viaduct in Tokyo[11]. The second type of organic inhibitors for EICI was quaternary ammonium salts, among which tetrabutylammonium bromide (TBAB) showed good performance in electrically-accelerated migration effectiveness[12, 13]. The imidazoline quaternary ammonium salt (IQS) was a corrosion inhibitor widely applied in petroleum industry[14, 15] and very recently, it was evaluated as electro-migrating inhibitor in reinforced concrete[16]. However, the reaction temperature for the synthesis of IQS corrosion inhibitor was up to 200 ^{o}C[17]. Thus, a more efficient route for the synthesis of novel quaternary ammonium salts with good inhibition effectiveness under mild reaction conditions remains highly desirable.In recent years, imidazolium quaternary ammonium salts, also called imidazolium ionic liquids have been regarded as green corrosion inhibitors for different metals and alloys in various aggressive media, particularly in acid solutions[18-30]. However, the effect of substituent in the imidazole ring on inhibitive performance remains unclear. One general accepted view was that imidazolium ionic liquids containing a longer alkyl chain exhibited higher corrosion efficiency probably because of their good hydrophobicity[31, 32]. Meanwhile, the research of imidazolium ionic liquids used as inhibitors for carbon steel in alkaline environments was very rare. The known example was reported by Yang group and they found that 1-butyl-3-methylimidazolium tetrafluoroborate could reduce the corrosion of carbon steel significantly[33]. Although pioneering work have been achieved in this field, the research on structure-activity relationship is superficial. Besides, the investigated imidazolium ionic liquids were limited to simple carbon chain substituted ones, which the inhibition effectiveness was mainly rely on hydrophobic effects rather than the electronic properties of the substituents. Considering that many inhibitors could absorb on metal surfaces via hydroxyls[33, 34], carboxyls[35, 36] or aromatic rings[37], imidazolium ionic liquids substituted with these polar groups (Fig. 1) may show better inhibitive performances.

Depending on the study of N-heterocycles[38, 39], we synthesize three imidazolium ionic liquids. We make fundamental evaluations of the corrosion inhibitive performance of steel reinforcement in the simulated concrete pore solution. On the other hand, imidazolium ionic liquids have advantages of good chemical stability and high ionic conductivity, promoting their potential application in electrical injection. Thus, their electrical migration capabilities are also assessed. The aim of this work is to study the role of polar substituents on inhibition effectiveness as well as electrical migration effectiveness.

2. EXPERIMENTAL

2.1 Synthesis of imidazolium ionic liquids

All reagents used in this study were purchased from commercial suppliers. ^{1}H NMR was conducted on a Bruker DPX 300 MHz spectrometer.

The imidazolium ionic liquids were prepared by two steps: nucleophilic substitution and cationized reaction, as shown in Fig. 1. The molecular structure of imidazolium ionic liquid is shown in Fig.2. The detailed process was described as followed.

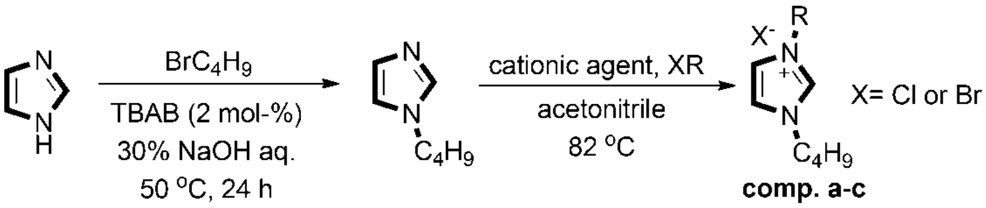

Figure 1. General procedure for synthesis of imidazolium ionic liquids.

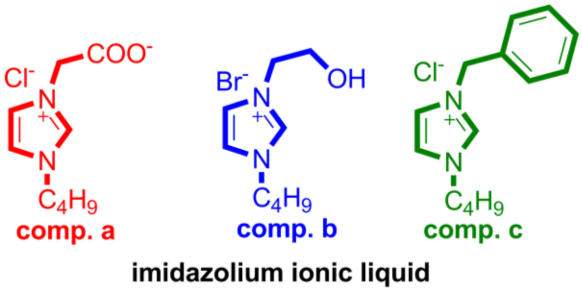

Figure 2. Molecular structures of imidazolium ionic liquid corrosion inhibitors.

N-butyl substituted imidazole: Imidazole (1.6 mol) and TBAB (2 mol-%) were dissolved in 30% NaOH aqueous solution (300 mL) under vigorous stirring, then 1-bromobutane (1.7 mol) was added dropwise at room temperature. The mixture was stirred at 50 °C for 24 h until two phases appear. Then the upper organic phase was extracted with ethyl acetate and washed with water and brine, then dried over anhydrous Na_2SO_4. The solvent was removed to give N-butyl substituted imidazole in quantitative yield and used without further purification.

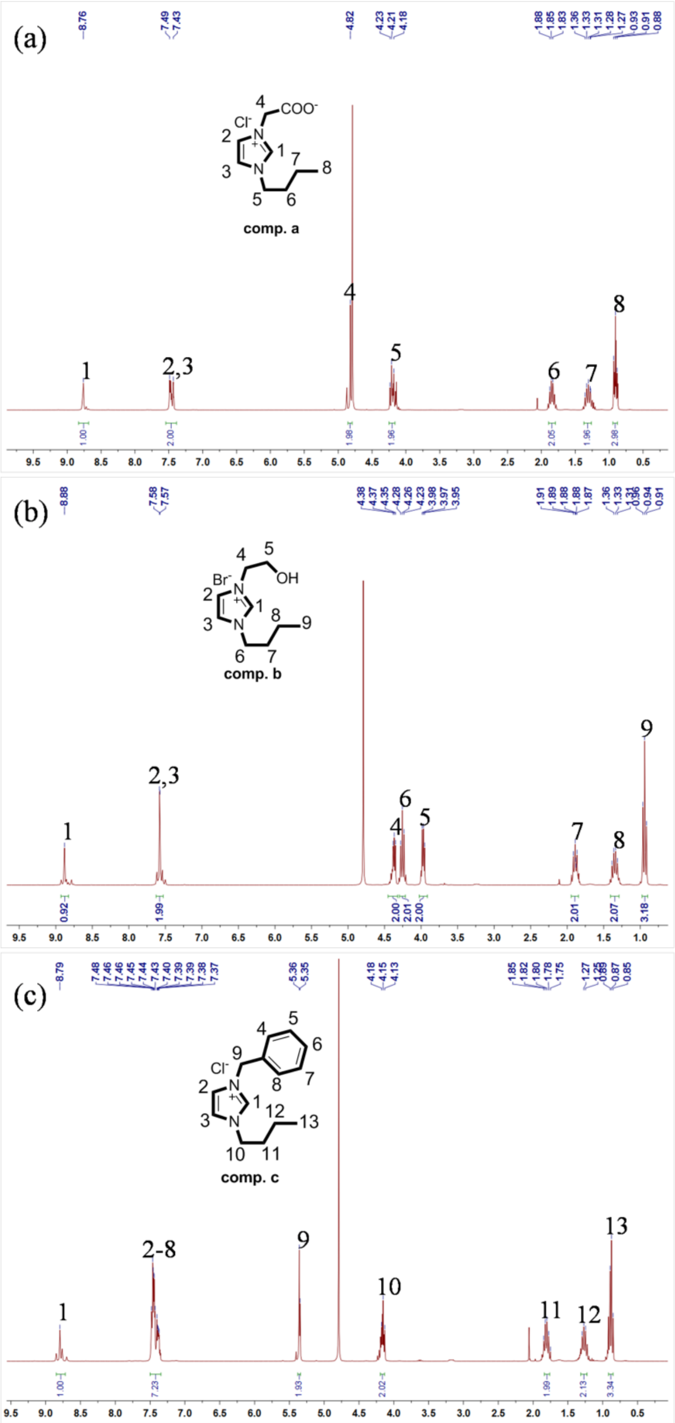

Figure 3. ^{1}H NMR spectra of imidazolium ionic liquids.

1-butyl-3-(carboxymethyl)-1H-imidazol-3-ium chloride (comp. a): The N-butyl substituted imidazole (0.3 mol) and sodium chloroacetate (0.3 mol) were dissolved in acetonitrile-water (volume ratio 1:1, 150 mL), and stirred at 82 °C for 24 h. The pH was kept in the range of 8-9 using 30% NaOH aqueous solution. After finished, the solvent was removed. The product was dissolved in anhydrous ethanol and the inorganic salt was removed by filtration. Then, ethanol was removed and the obtained oil was washed repeatedly with ethyl acetate and then dried under vacuum at 60 °C for 24 h (65%

yield). As shown in Fig. 3a, the ^{1}H NMR spectra showed the following signals: ^{1}H NMR (300 MHz, D_2O) δ 8.76 (s, 1H), 7.49 (s, 1H), 7.43 (s, 1H), 4.82 (s, 2H), 4.21 (t, *J* = 8.6 Hz, 2H), 1.89 – 1.82 (m, 2H), 1.37 – 1.26 (m, 2H), 0.91 (t, *J* = 7.4 Hz, 3H).

1-butyl-3-(2-hydroxyethyl)-1H-imidazol-3-ium bromide (comp. b): The N-butyl substituted imidazole (0.3 mol) and 2-bromoethanol (0.36 mol) were dissolved in acetonitrile (100 mL), and stirred at 82 °C for 24 h. After finished, the solvent was removed. The product was washed repeatedly with ethyl acetate and then dried under vacuum at 60 °C for 24 h (87% yield). As shown in Fig. 3b, the ^{1}H NMR spectra showed the following signals: ^{1}H NMR (300 MHz, D_2O) δ 8.88 (s, 1H), 7.58 (s, 1H), 7.57 (s, 1H), 4.39 – 4.33 (m, 2H), 4.26 (t, *J* = 7.1 Hz, 2H), 4.00 – 3.93 (m, 2H), 1.93 – 1.85 (m, 2H), 1.41 – 1.28 (m, 2H), 0.94 (t, *J* = 7.4 Hz, 3H).

3-benzyl-1-butyl-1H-imidazol-3-ium chloride (comp. c): The compound was prepared and purified similarly as comp. b, but benzyl chloride was used instead of 2-bromoethanol (78% yield). As shown in Fig. 3c, the ^{1}H NMR spectra showed the following signals: ^{1}H NMR (300 MHz, D_2O) δ 8.79 (s, 1H), 7.51 – 7.33 (m, 7H), 5.38 – 5.34 (m, 2H), 4.15 (t, *J* = 7.1 Hz, 2H), 1.87 – 1.74 (m, 2H), 1.32 – 1.23 (m, 2H), 0.87 (t, *J* = 6.4 Hz, 3H).

2.2 Materials and sample preparation

The simulated concrete pore solution was saturated $Ca(OH)_2$ solution with 0.3 M NaCl prepared by reagent grade chemicals and bi-distilled water and keep the pH at 12.5.

Working electrodes were prepared from the carbon steel bar. The composition of this steel is (in mass%): C 0.17, Mn 0.46, Si 0.26, Cu 0.019, S 0.017, P 0.0047 and Fe balance. Before tests, the working electrodes were burnished gradually with grit SiC paper (grade 240, 400, 1000 and 2000), then degreased and rinsed with acetone and ethanol.

Ordinary Portland cement P II 52.5 R was used to manufacture the cement mortar for electrical migration. In order to simulate poor quality concrete and effortless to suffer corrosion-induced deterioration, the cement mortar (100×100×300 mm) was made with the weight ratio of cement: sand: water of 1: 3: 0.6. The specimen was demoulded 1 day after casting and cured in a high humidity environment at room temperature for 3 months to ensure the mortar was thoroughly hydrated. After that, the specimen was cut into slabs with the dimensions of 100×100×10 mm.

2.3 Electrochemical measurements

The electrochemical measurements were performed in a three-electrode cell. Ag/AgCl electrode is the reference electrode, platinum mesh sheet is the counter electrode. Carbon steel is working electrode and exposed working area was 0.36 cm^2. All the electrochemical experiments were conducted on P4000 (Princeton Applied Research). The potentiodynamic polarization curves measurements were performed in the potential range from -200 to 800 mV versus the OCP with a scan rate of 0.5 mV/s after the electrodes were immersed in solutions for 1.0 h. Electrochemical impedance spectroscopy (EIS) was carried out at the open circuit potential (OCP) in the frequency range of 50 kHz-10 mHz with a 10 mV amplitude signal after the electrodes were immersed in simulated concrete pore solutions for 0.5h. EIS data was fitted using ZSimpWin software.

2.4 Surface analysis

The micrographies of the electrode surface were analyzed by scanning electron microscope (SEM, Quanta 250) at an acceleration voltage of 15 kV. Elemental analysis was performed with energy dispersive spectroscopy (EDS, Genesis Apollo X). The prepared working electrodes were immersed in 0.3 M NaCl saturated $Ca(OH)_2$ solutions with and without the inhibitor for 9d, respectively. After removal from the simulated concrete pore solution, the electrodes were rinsed with deionized water and dried with cool air.

3. RESULTS AND DISCUSSION

3.1 Electrochemical measurements

3.1.1 Potentiodynamic polarization curves (PDP)

In Fig. 4, it could be seen that in the presence of comp. a, the curves were shifted to lower current regions, suggesting the inhibition tendency of the imidazolium ionic liquid. The corrosion potential moved positively when comp. a was added, while there were no definite trend in the value shift.

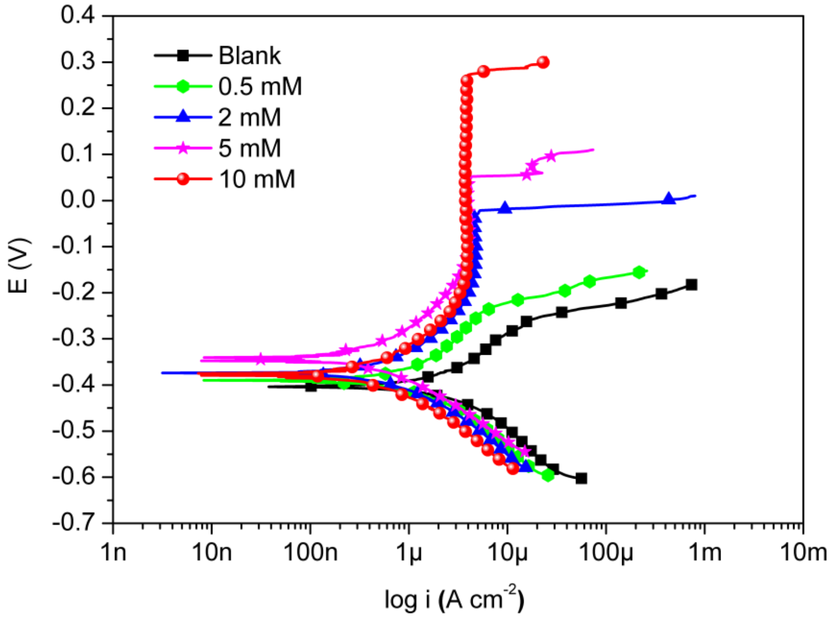

Figure 4. Potentiodynamic polarization curves for carbon steel in 0.3 M NaCl sat. $Ca(OH)_2$ solutions without and with different concentrations of comp. a.

Table 1. The electrochemical parameters estimated from PDP data for carbon steel in 0.3M NaCl sat. $Ca(OH)_2$ solutions with different concentrations of comp. a

Conc. (mM)	E_{corr} (mv)	E_{pit} (mv)	$-\beta_c$ (mV dec^{-1})	β_a (mV dec^{-1})	I_{corr} (μA cm^{-2})	θ	IE (%)
Blank	-401	—	208	244	4.01	—	—
0.5	-386	—	177	242	1.54	0.616	61.6
2	-374	-22	165	254	0.926	0.769	76.9
5	-342	52	144	236	0.618	0.846	84.6
10	-377	273	153	214	0.596	0.851	85.1

Table 1 collects the electrochemical parameters from polarization curves, including the values of corrosion potential (E_{corr}), cathodic (β_c) and anodic (β_a) slops. In this study, the degree of surface coverage (θ) is approximate considered equal to inhibition efficiency (IE), and calculated by the following equations:

$$\theta = \frac{i^0_{corr} - i_{corr}}{i^0_{corr}} \qquad (1)$$

$$IE = \frac{i^0_{corr} - i_{corr}}{i^0_{corr}} \times 100\% \qquad (2)$$

Where, i^0_{corr} and i_{corr} were the corrosion current densities for electrode without and with inhibitor, respectively.

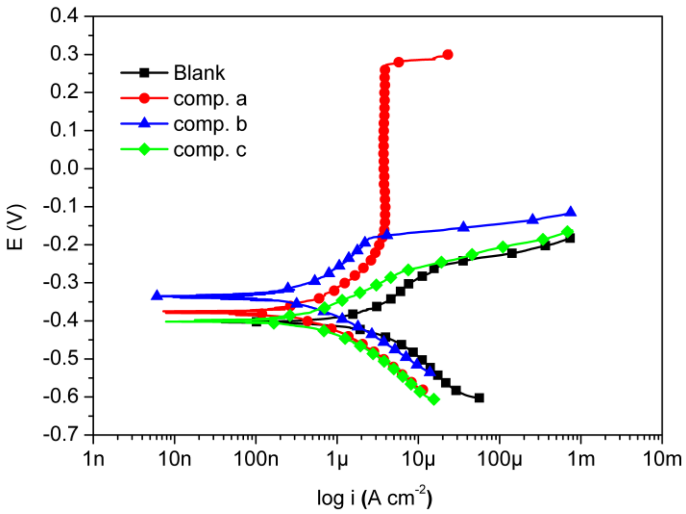

Figure 5. Potentiodynamic polarization curves for carbon steel in 0.3 M NaCl sat. $Ca(OH)_2$ solutions without and with 10 mM different imidazolium ionic liquids.

The shift in E_{corr} values was in the range of less than 85 mV, suggesting this compound was a mixed type of inhibitor.[40] Notably, β_a values changed slightly with the increasing concentration of inhibitor, while β_c displayed more pronounced change. The results suggested that the inhibitor reduced the anodic oxidation reaction of iron meanwhile restrained the oxygen reduction reaction, but the latter effect seemed more prominent. The pitting potential (E_{pit}) represented anodic breakdown potential, at which suddenly rise in current density took place. As the concentration of inhibitor increased, E_{pit} shifted to the positive direction, due to the formation of a more stable and density barrier film on the electrode surface[41].

Table 2. The electrochemical parameters estimated from PDP data for carbon steel in 0.3M NaCl sat. $Ca(OH)_2$ solutions without and with 10 mM different inhibitors

Comp.	E_{corr} (mv)	E_{pit} (mv)	$-\beta_c$ (mV dec^{-1})	β_a (mV dec^{-1})	I_{corr} (μA cm^{-2})	IE (%)
Blank	-401	—	208	244	4.01	—
comp. a	-377	273	153	214	0.596	85.1
comp. b	-334	—	129	193	0.446	88.9
comp. c	-402	—	137	141	0.708	82.3

Then, other imidazolium ionic liquids at the concentration of 10 mM were tested through PDP curves. The results and fitted parameters were presented in Fig. 5 and Table 2, respectively. It was readily apparent that E_{pit} of comp. a inhibited conditions had a significantly positive value, while no obvious anodic breakdown potential was obtained from comp. b or comp. c inhibited curves. It was reported that carboxylates adsorbed on metal surface through the delocalised electrical charge on the two oxygen atoms of the carboxylic group, resulting in higher E_{pit} value than other commonly used organic inhibitors, such as amines and alkanolamines[42]. Considering that the strong link between inhibiting properties and molecular structures, the present results confirmed the similar structure-activity relationship. According to test results, comp. b with a hydroxyl in molecular structure reached the best inhibition efficiency. We speculated the adsorption probably occur through the π electrons of the imidazole ring and the free lone-pair electrons of heteroatoms (nitrogen and oxygen), while the alkyl chain of C_4 played a sort of physical barrier against chloride migration towards the steel surface. Since the alkyl chain was same, the adsorption of inhibitors depended closely on the steric effects as well as electronic properties of these polar substituents.

3.1.2 Electrochemical impedance spectroscopy

EIS studies were further conducted to investigate corrosion inhibition process of comp.a, because of comp. a showed the best performance against the chloride-induced protective film breakdown. Fig.6 presents the influence of concentration of comp.a on the corrosion behaviour of electrode by EIS polts. The results show that the arc radiuses increase significantly with the concentration of comp.a and larger that blank sample, which demonstrated that the protective film formed on steel surface and gradually became more and more density with increasing the inhibitor concentration. The appearance of the inductive shrinkage in the low frequency range was attributed to the relaxation process obtained by adsorption species such as Cl^- or adsorption-desorption process of the inhibitor on steel surface[19, 43]. Therefore, this inductive arc was disregarded in the following equivalent circuit. In Bode plots, impedance modulus at low frequency of the inhibited systems increased as the concentration of inhibitor increase, which indicated the corrosion of electrode was restricted by the inhibitor. On the contrary, the impedance modulus at low frequency was about five times greater than that in the blank solution even though the concentration of inhibitor was only 10 mM. Besides, phase angles of electrode inhibited by inhibitor moved to lower frequencies, which demonstrated that coverage of electrode surface increase with the adsorption of inhibitor molecular and/or with the deposition of products[33].

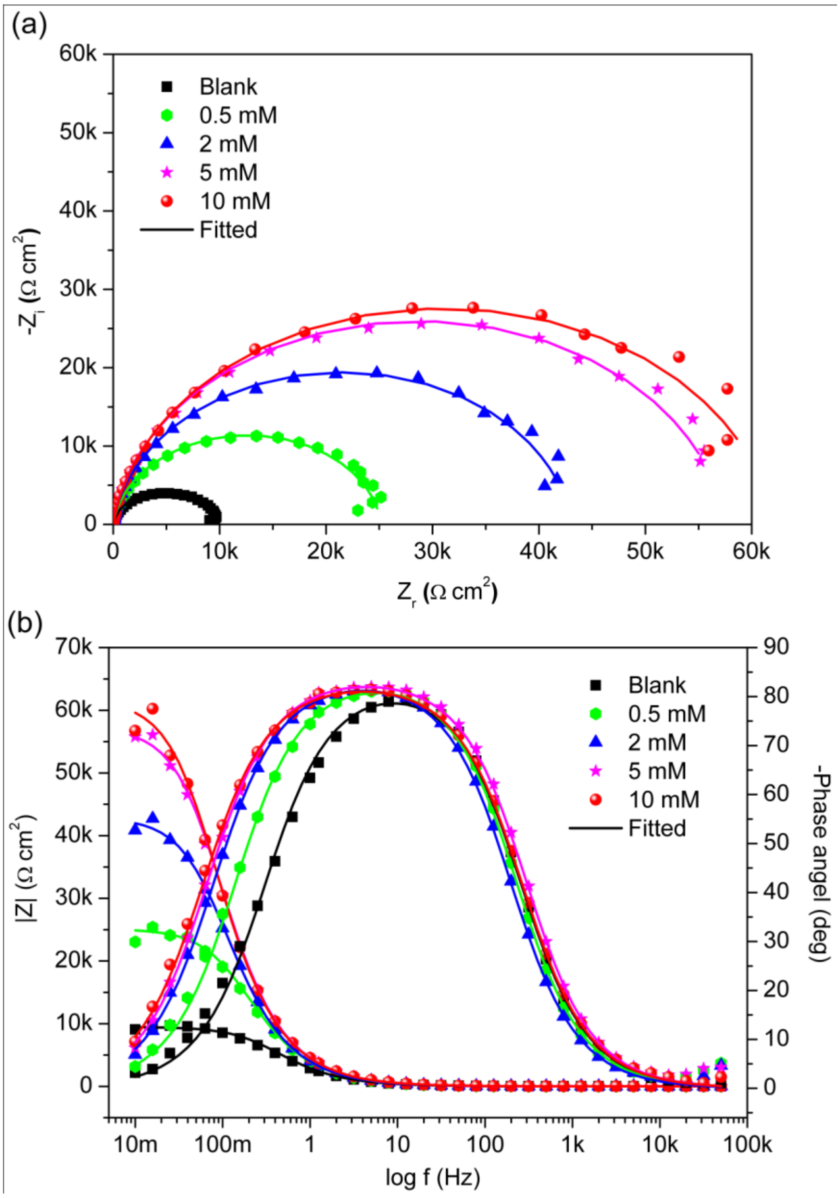

Figure 6. (a) Nyquist and (b) Bode plots for carbon steel in 0.3 M NaCl sat. $Ca(OH)_2$ solutions without and with different concentrations of comp. a.

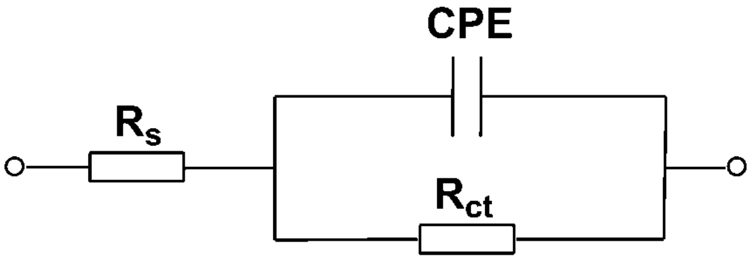

Figure 7. Electrochemical equivalent circuit.

The EIS results could be elucidated by equivalent circuit. As shown in Fig. 7, the equivalent circuit for fitted the EIS is consist of one time constant. In this circuit, R_s represented the electrolyte resistance, R_{ct} represented the charge transfer resistance and the constant phase element CPE was used to instead of the double layer capacitance (C_{dl}).

Table 3. The fitted electrochemical parameters from EIS for carbon steel in 0.3 M NaCl sat. $Ca(OH)_2$ solutions with different concentrations of comp. a

Conc. (mM)	R_s (Ω cm^2)	R_{ct} (Ω cm^2)	C_{dl} (μF cm^{-2})	n	ChiSq (10^{-3})	θ	IE%
Blank	18.12	9487	57.36	0.93	1.46	—	—
0.5	24.66	25150	44.54	0.94	1.60	0.623	62.3
2	28.78	43020	44.56	0.93	1.04	0.779	77.9
5	22.14	57430	39.02	0.94	1.13	0.835	83.5
10	25.73	61970	40.14	0.93	0.804	0.847	84.7

The corresponding impedance parameters were listed in Table 3. θ and IE were calculated by the following equations:

$$\theta = \frac{R_{ct} - R_{ct}^0}{R_{ct}} \quad (3)$$

$$IE = \frac{R_{ct} - R_{ct}^0}{R_{ct}} \times 100\% \quad (4)$$

Where, R_{ct}^0 and R_{ct} were the charge transfer resistances of electrodes in solution without and with inhibitor, respectively. The quality of the fitted result calculated from the equivalent circuit was judged by the ChiSq value, and lower values indicated the results fitted very well with the measured parameters. It was obviously that C_{dl} tended to decrease with the inhibitor added to blank solution. Meanwhile, R_{ct} increased significantly with the increase of inhibitor concentration. The inhibition efficiency calculated from EIS was in good agreement with that from potentiodynamic polarization curves measurements.

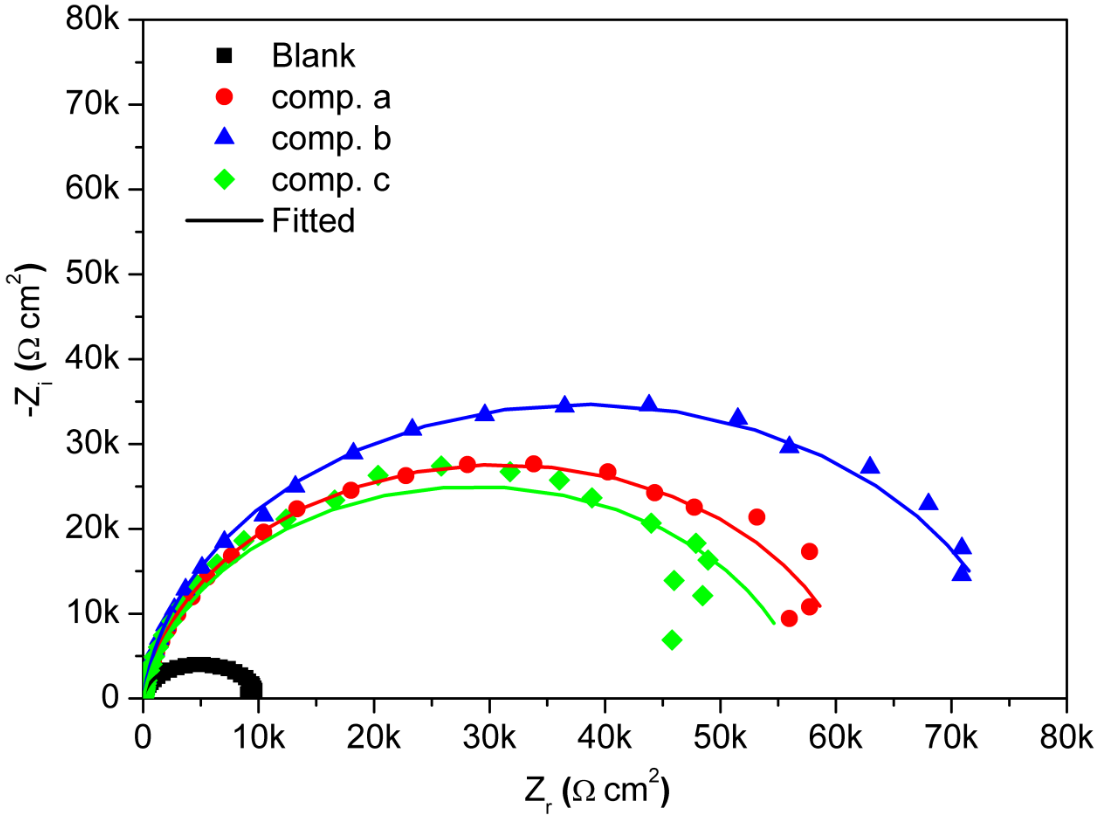

Figure 8. Nyquist plots for carbon steel in 0.3 M NaCl sat. $Ca(OH)_2$ solutions without and with 10 mM different imidazolium ionic liquids.

The EIS results were further obtained for steel electrodes in solutions with 10 mM comp. b and comp. c, as shown in Fig. 8. The inductive shrinkage was also detected, but this phenomenon gradually disappeared with the capacitive arc increased. The results indicated that less amount of Cl^- absorbed on the steel surface because of the formation of a more density and stable adsorption film. The data listed in Table 4. also suggested that the inhibitors followed the order comp. b > comp. a > comp. c in terms of inhibitive effectiveness.

Table 4. The fitted electrochemical parameters from EIS for carbon steel in 0.3 M NaCl sat. $Ca(OH)_2$ solutions without and with 10 mM different inhibitors

Comp.	R_s (Ω cm^2)	R_{ct} (Ω cm^2)	C_{dl} (μF cm^{-2})	n	ChiSq (10^{-3})	IE%
Blank	18.12	9487	57.36	0.93	1.46	—
comp. a	25.73	61970	40.14	0.93	0.804	84.7
comp. b	23.83	76190	38.15	0.94	1.10	87.5
comp. c	24.20	57330	36.63	0.91	2.75	83.5

3.2 Adsorption isotherm

To make the adsorption process more clear, we selected comp. a to calculate adsorption isotherms. The adsorption of comp. a obeyed the Langmuir adsorption isotherm[44], and the θ was related to inhibitor concentration C, the formula of Langmuir adsorption isotherm is as follow:

$$\frac{C}{\theta} = \frac{1}{K_{ads}} + C \quad (5)$$

where K_{ads} was the adsorption equilibrium constant.

θ is calculated by electrochemical measurements of PDP and EIS, the relative results were shown in Table 1 and Table 3.

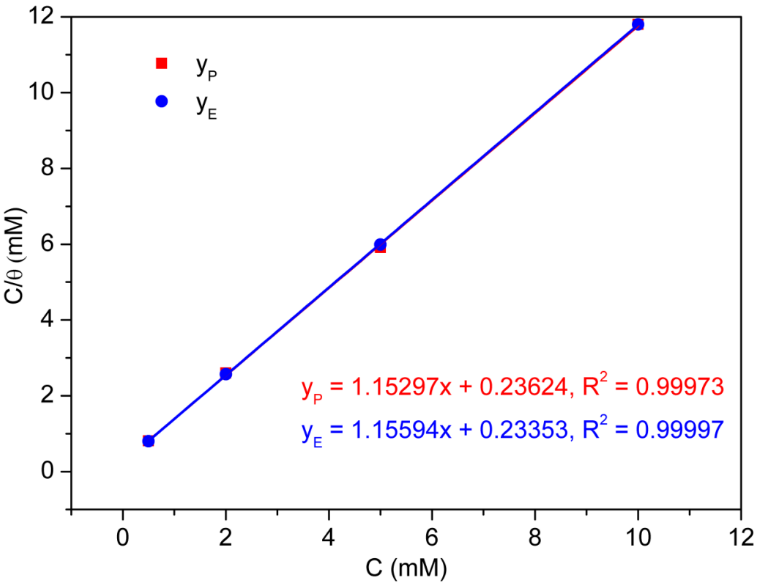

Figure 9. Langmuir adsorption isotherm of comp. a on carbon steel surface.

The relationship between C/θ and C was presented in Fig. 9. The subscripts of fitting fumula of P and E represented the data calculted form PDP and EIS measurements, respectively. The correlation coefficient R^2 and line slope were close to 1, affirming the good consistency between experimental results and theoretical simulation. The related standard free energy of adsorption ΔG^0_{ads} could be estimated by the following equation:

$$K_{ads} = \frac{1}{55.5} \exp\left(- \frac{\Delta G^0_{ads}}{RT} \right) \quad (6)$$

Where, the value of 55.5 was the concentration of water in solution expressed in moles, R was the universal gas constant, and T was the absolute temperature (298 K in present study).

Table 5. Thermodynamic parameters for the adsorption of comp. a on carbon steel in 0.3 M NaCl sat. $Ca(OH)_2$ solutions

Method	K_{ads} (L mol^{-1})	ΔG^0_{ads} (kJ mol^{-1})
PDP	4.23×10^3	-30.6
EIS	4.28×10^3	-30.7

Table 5 shows the thermodynamic parameterscalculated by the formlation of (6). The high negative values of ΔG^{0}_{ads} indicated that adsorption process occurred spontaneously. Generally, the value of ΔG^{0}_{ads} up to -20 kJ mol^{-1} was consistent with the electrostatic interaction between the charged molecule and the charged metal (physical adsorption), while negative than -40 kJ mol^{-1} involved sharing or transferring of electrons between the inhibitor molecule with the metal surface to form a coordinate type bond (chemical adsorption)[45]. In present research, both chemical and physical adsorption processes occurred on the electrode surface.

3.3. Surface analysis

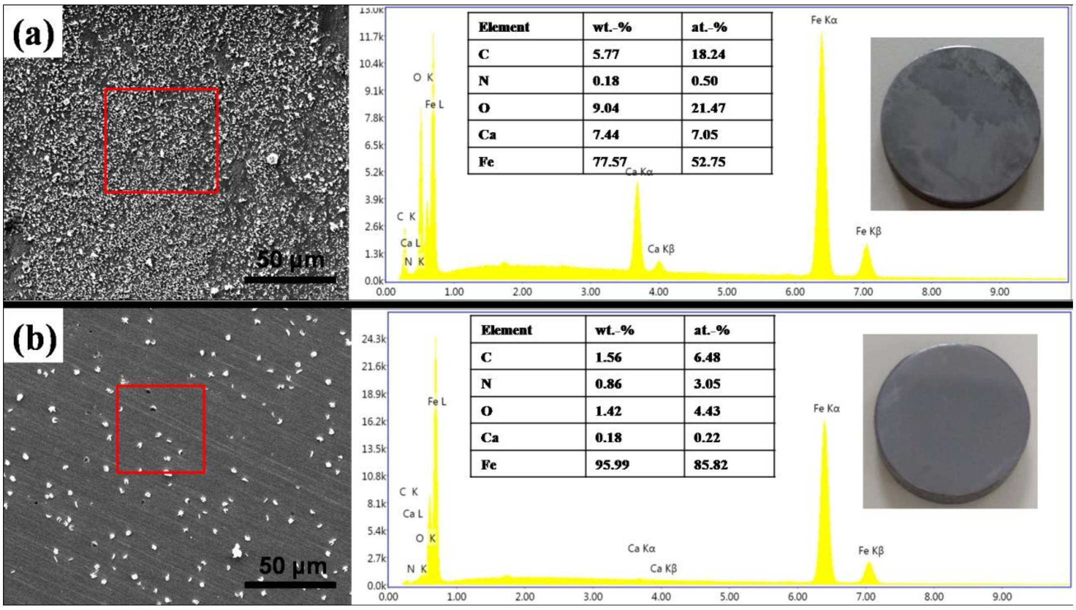

Element	**wt.-%**	**at.-%**
C	**5.77**	**18.24**
N	**0.18**	**0.50**
O	**9.04**	**21.47**
Ca	**7.44**	**7.05**
Fe	**77.57**	**52.75**

Element	**wt.-%**	**at.-%**
C	**1.56**	**6.48**
N	**0.86**	**3.05**
O	**1.42**	**4.43**
Ca	**0.18**	**0.22**
Fe	**95.99**	**85.82**

Figure 10. Morphological observation of the steel surface via SEM and EDS analysis (a) without inhibitor; (b) with 10 mM comp. a, where the photographs of steel electrodes are also present.

In order to further examine the corrosion behaviour of steel in simulated pore solution contaminated by chloride ion, the SEM and EDS was conducted. Fig.10 displays the surface micro-topography of steel erosion in solution contaminated by chloride ion with and without inhibitors. Visual inspection showed the steel in the blank solution suffered from a severe corrosion damage which was also confirmed by micrographs. While in inhibited solution, a cleaner and smoother surface was observed.

The detailed surface analysis via EDS showed the mainly elements on steel surface. As shown in Fig.10, the scanning area was marked out in the SEM image. The characteristics peaks of the selected elements, including Fe, C, N, O and Ca, and the exact content was also listed. The total element content was normalized to 100%. The higher concentrations of C, O and Ca and lower concentration of Fe were detected for the steel in blank solution, suggesting the white deposition layer covered on steel surface contained $CaCO_3$. Meanwhile, the content of N increased obviously under inhibited conditions, which was vital evidence of imidazolium ionic liquid absorbed on the steel surface.

4. CONCLUSIONS

In summary, imidazolium ionic liquids substituted with both polar groups and alkyl chains have been synthesized. We also made fundamental study on their corrosion inhibitive performances of carbon steel in alkaline chloride solution using electrochemical techniques as well as surface analysis. Moreover, a preliminary research on the migration of imidazolium ionic liquids was carried out under action of electric field.

Based on the experimental data, the following conclusions can be drawn:

(1) Imidazolium ionic liquid acted as a mixed type of inhibitor could effectively suppress the localised corrosion of steel in concentration dependent manner.

(2) The adsorption of comp. a corresponded well with Langmuir isotherm and the calculated thermodynamic parameters indicated both physical and chemical adsorption on the steel surface.

(3) The visual inspection and SEM analysis verified that imidazolium ionic liquid could effectively inhibit the formation of corrosion product on the steel surface. The inhibition performance was probably attributed to the absorption of inhibitor, which was verified by EDS analysis.

ACKNOWLEDGEMENTS
This work was supported by the National Key R & D Program of China (No. 2017YFB0309904), NSFC-ShanDong union （U1706222）, National Natural Science Foundation of China (No. 51908254) and Natural Science Foundation of Jiangsu Province of China (BK20160104, BK20171111), Jiangsu Key R & D Program(BE2017158), Six Peak Talents Programs(XCL-115).

References

1. I. Vyrides, E. Rakanta, T. Zafeiropoulou, G. Batis, *Open J. Civ. Eng.*, 3 (2013) 1.
2. H. Zheng, W. Li, F. Ma, Q. Kong, *Cem. Concr. Res.*, 55 (2014) 102.
3. L. Holloway, K. Nairn, M. Forsyth, *Cem. Concr. Res.*, 34 (2004) 1435.
4. H.E. Jamil, A. Shriri, R. Boulif, M.F. Montemor, M.G.S. Ferreira, *Cem. Concr. Compos.*, 27 (2005) 671.
5. H.B. Zheng, W.H. Li, F.B. Ma, Q.L. Kong, *Constr. Build. Mater.*, 37 (2012).
6. S. Sawada, C.L. Page, M.M. Page, *Corros. Sci.*, 47 (2005) 2063.
7. Y.J. Liu, X.M. Shi, *Corros. Rev.*, 27 (2009)53.
8. S. Sawada, J. Kubo, C.L. Page, M.M. Page, *Corros. Sci.*, 49 (2007)1186.
9. J. Kubo, S. Sawada, C.L. Page, M.M. Page, *Mater. Corros.*, 59 (2008) 107.
10. C. Xu, W.L. Jin, H.L. Wang, H.T. Wu, N. Huang, Z.Y. Li, J.H. Mao, *Constr. Build. Mater.*, 115 (2016) 602.
11. J. Kubo, Y. Tanaka, C.L. Page, M.M. Page, *Constr. Build. Mater.*, 39 (2013) 2.
12. T.H. Nguyen, T.A. Nguyen, T.V. Nguyen, V.K. Le, T.M.T. Dinh, H. Thai, X. Shi, *International*

Journal of Corrosion, 2015 (2015) 1.
13. T. Pan, T.A. Nguyen, X. Shi, *Transport. Res. Rec.: J. Transport. Res. Board.*, 2044 (2008) 51-60.
14. P.C. Okafor, Y. Zheng, *Corros. Sci.*, 51 (2009) 850.
15. F.L. Zeng, X. Tan, J.F. Li, Z. Zhang, *Corros. Eng. Sci. Techn.*, 48 (2013) 108.
16. F.L. Fei, J. Hu, Q.J. Yu, J.X. Wei, Y.B. Nong, *Mater. Corros.*, 66 (2015) 1039.
17. F.L. Fei, J. Hu, J.X. Wei, Q.J. Yu, Z.S. Chen, *Constr. Build. Mater.*, 70 (2014) 43.
18. N.V. Likhanova, M.A. Dominguez-Aguilar, O. Olivares-Xometl, N. Nava-Entzana, E. Arce, H. Dorantes, *Corros. Sci.*, 52 (2010) 2088.
19. X. Zheng, S. Zhang, W. Li, M. Gong, L. Yin, *Corros. Sci.*, 95 (2015) 168.
20. A.P. Hanza, R. Naderi, E. Kowsari, M. Sayebani, *Corros. Sci.*, 107 (2016) 96.
21. X.W. Zheng, S.T. Zhang, M. Gong, W.P. Li, *Ind.Eng. Chem. Res.*, 53 (2014) 16349.
22. H. Ashassi-Sorkhabi, M. Es'haghi, *Mater. Chem. Phys.*, 114 (2009) 267.
23. K. Zhang, W. Yang, C. Yun, B. Xu, X. Yin, L. Ying, H. Zuo, *J. Mater. Sci.*,53 (2018) 14666.
24. C. Verma, I.B. Obot, I. Bahadur, E.S.M. Sherif, E.E. Ebenso, *Appl. Surf. Sci.*, 1 (2018) 134.
25. G. Vastag, A. Shaban, M. Vraneš, A. Tot, S. Belić, S. Gadžurić, *J. Mol. Liq.*, 264 (2018) 526.
26. F. Li, S. Zhang, Y. Qiang, S. Xu, B. Tan, S. Chen, *Mater. Chem. Phys.*, 215 (2018) 219.
27. F. El-Hajjaji, M. Messali, A. Aljuhani, M.R. Aouad, B. Hammouti, M.E. Belghiti, D.S. Chauhan, M.A. Quraishi, *J. Mol. Liq.*, 249 (2018) 997.
28. Y. Qiang, S. Zhang, G. Lei, X. Zheng, B. Xiang, S. Chen, *Corros. Sci.*, 119 (2017) 68.
29. M.A. Migahed, M.M. El-Rabiei, H. Nady, H.M. Gomaa, E.G. Zaki, *J. Bio. Trib. Corros.*, 3 (2017) 22.
30. M.A. Deyab, M.T. Zaky, M.I. Nessim, *J. Mol. Liq.*, 229 (2017) 396.
31. D. Guzman-Lucero, O. Olivares-Xometl, R. Martinez-Palou, N.V. Likhanova, M.A. Dominguez-Aguilar, V. Garibay-Febles, *Ind.Eng. Chem. Res.*, 50 (2011) 7129.
32. L.C. Murulana, A.K. Singh, S.K. Shukla, M.M. Kabanda, E.E. Ebenso, *Ind.Eng. Chem. Res.*, 51 (2012) 13282.
33. X. Zhou, H.Y. Yang, F.H. Wang, *Acta Phys.-Chim. Sin.*, 27 (2011) 647.
34. X. Zhou, H. Yang, F. Wang, *Corros. Sci.*, 54 (2012) 193.
35. J.H. Li, B. Zhao, J. Hu, H. Zhang, S.G. Dong, R.G. Du, C.J. Lin, *International Journal of Electrochemical Science*, 10 (2015) 956.
36. M. Ormellese, F. Bolzoni, L. Lazzari, A. Brenna, M. Pedeferri, *Mater. Corros.*, 62 (2011) 170.
37. N. Kicir, G. Tansug, M. Erbil, T. Tuken, *Corros. Sci.*, 105 (2016) 88.
38. D. Zhao, Q. Shen, J.X. Li, *Adv. Synth. Catal.*, 357 (2015) 339.
39. D. Zhao, T. Wang, Q. Shen, J.X. Li, *Chem. Commun.*, 50 (2014) 4302.
40. N. Soltani, N. Tavakkoli, M. Khayatkashani, M.R. Jalali, A. Mosavizade, *Corros. Sci.*, 62 (2012) 122.
41. H.E. Jamil, M.F. Montemor, R. Boulif, A. Shriri, M.G.S. Ferreira, *Electrochim. Acta*, 48 (2003) 3509.
42. M. Ormellese, L. Lazzari, S. Goidanich, G. Fumagalli, A. Brenna, *Corros. Sci.*, 51 (2009) 2959.
43. M. El Achouri, M.R. Infante, F. Izquierdo, S. Kertit, H.M. Gouttaya, B. Nciri, *Corros. Sci.*, 43 (2001) 19.
44. M.S. Morad, *J. Appl. Electrochem.*, 38 (2008) 1509.
45. M. Bouklah, B. Hammouti, M. Lagrenée, F. Bentiss, *Corros. Sci.*, 48 (2006) 2831.
46. L. Valek, S. Martinez, D. Mikulić, I. Brnardić, *Corros. Sci.*, 50 (2008) 2705.